AIP | Journal of Applied Physics

Structure and dielectric properties of (Sr1−1.5xBix)TiO3 thin films

Peng Shi, Wei Ren, Min Zhao, Xiaoyong Wei, Xiaoqing Wu et al.

Citation: J. Appl. Phys. **105**, 084104 (2009); doi: 10.1063/1.3106162
View online: http://dx.doi.org/10.1063/1.3106162
View Table of Contents: http://jap.aip.org/resource/1/JAPIAU/v105/i8
Published by the AIP Publishing LLC.

Structure and dielectric properties of $(Sr_{1-1.5x}Bi_x)TiO_3$ thin films

Peng Shi,[a] Wei Ren, Min Zhao, Xiaoyong Wei, Xiaoqing Wu, Xiaofeng Chen, and Xi Yao
Electronic Materials Research Laboratory, Key Laboratory of the Ministry of Education, Xi'an Jiaotong University, Xi'an 710049, China

(Received 16 October 2008; accepted 21 February 2009; published online 20 April 2009)

Bismuth doped $SrTiO_3$ material has shown very interesting phenomena. Dielectric and ferroelectric relaxations have been recently reported in bismuth doped $SrTiO_3$ ceramics in the lower temperature range. Thin films of bismuth doped $SrTiO_3$ $[(Sr_{1-1.5x}Bi_x)TiO_3]$ $(x=0.0, 0.05, 0.10)$ have been prepared by a sol-gel method and investigated in this work. The phases and surface morphologies of thin films were analyzed to assess the structures and crystallization. The structure of the thin films is revealed as a cubic perovskite structure with no other phase detected. The dielectric properties and dielectric tunability of $(Sr_{1-1.5x}Bi_x)TiO_3$ thin films have been studied as a function of doping amount of bismuth and discussed in detail. © *2009 American Institute of Physics*.
[DOI: 10.1063/1.3106162]

I. INTRODUCTIONS

$SrTiO_3$ (STO) is an intrinsic quantum paraelectric.[1] However, it is reported that ferroelectric order can be induced in STO by the application of external electrical fields or mechanical stresses[2] or by introducing substitutional defects[3,4] into the lattice, such as Bi, Ca, etc. Bismuth doped $SrTiO_3$ $[(Sr_{1-1.5x}Bi_x)TiO_3]$ material has been studied since the 1950s and has shown very interesting phenomena.[4,5] It is revealed in x-ray analysis performed down to liquid nitrogen temperatures that the doped $SrTiO_3$ could maintain the single-phase perovskite structure for $x<20\%$.[6] Moreover, Yu and co-workers[5–10] observed the coexistence of several dielectric peaks with different physical characteristics in Bi doped $SrTiO_3$, such as the oxygen vacancies related relaxations at higher temperature and evolution from "dielectric relaxor" to "ferroelectric relaxor" at lower temperature in Bi doped $SrTiO_3$ materials, while the doped Bi concentration is lower than 10%, indicating the complexity of the doping effect in the quantum paraelectric $SrTiO_3$. In our previous work,[11] it is found that Bi impurity can induce ferroelectricity and the tunability in $SrTiO_3$ ceramic remarkably while the doped Bi concentration is within 10%. The tunability of the samples above 10% Bi concentration becomes very weak drastically and the values are smaller than 1% with a trend of linear decreasing. At the same time, ferroelectricity of the system is weak gradually for the samples above 10% Bi concentration.[11] The anomalies phenomena may be contributed by the formation of several kinds of polar clusters[8] or superparaelectricity[4] after introducing bismuth in $SrTiO_3$.

Moreover, Bi-doped $SrTiO_3$ is emerging as one of the promising materials for microwave dielectric tunable devices owing to their relatively large figures of merit.[7,11] However, there are few reports on the tunability and the dielectric property for Bi-doped $SrTiO_3$ thin films. In this paper, pure $SrTiO_3$, 5 mol % Bi, and 10 mol % Bi doped $SrTiO_3$ thin films, summarized as $[(Sr_{1-1.5x}Bi_x)TiO_3]$ $(x=0.0, 0.05, 0.10)$, were prepared by a sol-gel method. The structure and dielectric properties were investigated. The dielectric tunability as a function of temperature and frequency was also investigated in order to understand the effect of Bi content on the tunability of Bi-doped $SrTiO_3$ thin films.

II. EXPERIMENTAL PROCEDURE

The precursor solutions were prepared according to a nominal stoichiometry of $[(Sr_{1-1.5x}Bi_x)TiO_3]$ (BiST) $(x=0.0, 0.05, 0.1)$. For the synthesis of BiST sols, strontium acetate $(Sr(CH_3COO)_2\cdot 1/2H_2O)$, bismuth nitrate $[Bi(NO_3)_3\cdot 5H_2O]$, and tetrabutyl titanate $[Ti(OC_4H_9)_4]$ were used as starting materials. Glacial acetic acid $[CH_3COOH]$ and ethylene glycol monoethyl ether $[CH_3OCH_2CH_2OH]$ were used as solvents. First, strontium acetate and bismuth nitrate were dissolved in acetic acid and heated to 115 °C for 20 min, respectively, and then mixed together to form Bi–Sr mixture solutions under 60 °C with continuous stirring. Tetrabutyl titanium and acetylacetone with a mole ratio of 1:2 were dissolved in ethylene glycol monoethyl ether with constant stirring for 30 min at room temperature. Then, the Bi–Sr solutions were added to Ti solution via drop by drop. The final mixture has been stirred for additional 2 h to get a homogeneous precursor solution of BiST. The concentration of solution was adjusted to approximately 0.4 mol/L by adding ethylene glycol monoethyl ether.

BiST wet films were prepared on $Pt/Ti/SiO_2/Si(100)$ substrate by a spin-coating process at 3000 rpm for 30 s. The wet films were gone through a thermal treatment at 400 °C for 3 min and 700 °C for 5 min sequentially by a rapid thermal annealing method. The process of spin coating/thermal annealing was repeated six times to prepare thicker films.

The surface states of each element in BiST films were examined by an ESCALAB MK-II x-ray photoelectron spectroscopy (XPS). Phase composition, microstructure, and crystallization behavior of BiST films were investigated by a Rigaku D/MAX-2400 x-ray diffractometer (XRD), a VEECO dimension 3100 atomic force microscope (AFM), and a JEOL JSM-6700F field-emission scanning electron mi-

[a]Electronic mail: spxjy@mail.xjtu.edu.cn.

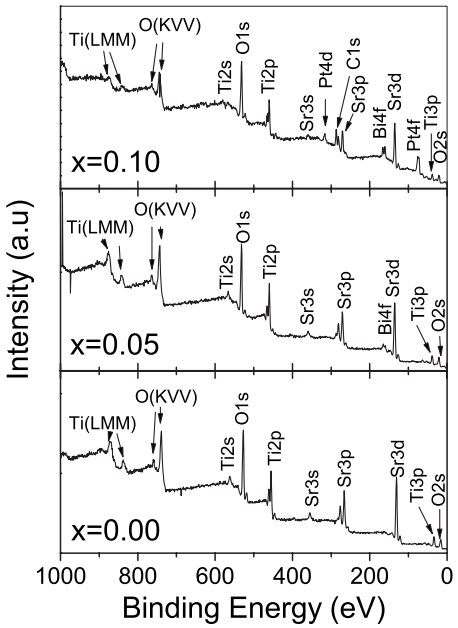

FIG. 1. XPS survey spectra of each element in BiST films surface (x=0,0.05,0.10).

croscope (FESEM), respectively. The thickness of the films was measured and calculated from cross-section FESEM images. For electric measurements, 1-mm-diameter upper gold electrodes were deposited by a sputtering method on the surface of the thin films using a shadow mask to form a metal-ferroelectric-metal (MFM) configuration. The dielectric properties and tunability as a function of frequency and temperature were measured with an Agilent 4294A precision impedance analyzer.

III. RESULTS AND DISCUSSION

Figure 1 shows XPS survey spectra of the BiST films. There are XPS photoelectron peaks and the corresponding Auger lines of Sr, Ti, O, Bi, and C elements on the film surface. The C 1*s* peak located at 284.6 eV is used as the criterion to rectify the binding energy of XPS spectra. Characteristic photoelectron peaks for Ti 2*s*, Ti 2*p*, Ti 3*p*, Sr 3*s*, Sr 3*p*, Sr 3*d*, C 1*s*, O 1*s*, O 2*s*, Bi 4*f*, and Auger peaks for Ti (LMM), and O (KVV) are identified in Fig. 1,[12] respectively. It can be seen that the signal of the Bi element appears in the Bi-doped $SrTiO_3$ film.

Figure 2 shows the narrow-scan spectra of the Sr 3*d*, Ti 3*p*, O 1*s*, and Bi 4*f* peaks for the $(Sr_{1-1.5x}Bi_x)TiO_3$ (x=0,0.05,0.1) thin films, respectively. The Sr 3*d* narrow-scan spectra, fitted by Gaussain multipeaks fit method, of the BiST films are shown in Fig. 2(a). The subpeaks located at 132.29 and 133.92 eV for x=0.00, at 131.65 and 133.22 eV for x=0.05, and at 131.60 and 133.18 eV for x=0.10 are ascribed to Sr $(3d_{5/2})$–O and Sr $(3d_{3/2})$–O bonds, respectively. Spin-orbit splitting energy of the pure Sr 3*d* doublet is about 1.6 eV, which indicates that the chemical state of Sr is Sr^{2+} on the basis of the principle and instrument handbook of XPS.[12]

Figure 2(b) shows the Ti 3*p* narrow-scan spectra of the films. The doublet peaks of 457.90 and 463.90 eV for x=0.00, 457.62 and 463.62 eV for x=0.05, and 457.55 and 463.35 eV for x=0.10 are mainly identified as the signal from Bi$(3p_{5/2})$–O and Bi$(3p_{3/2})$–O bonds. Spin-orbit splitting energy of the doublet is about 6.0 eV, indicating that the Ti element mainly exists as the chemical state of Ti^{4+}.

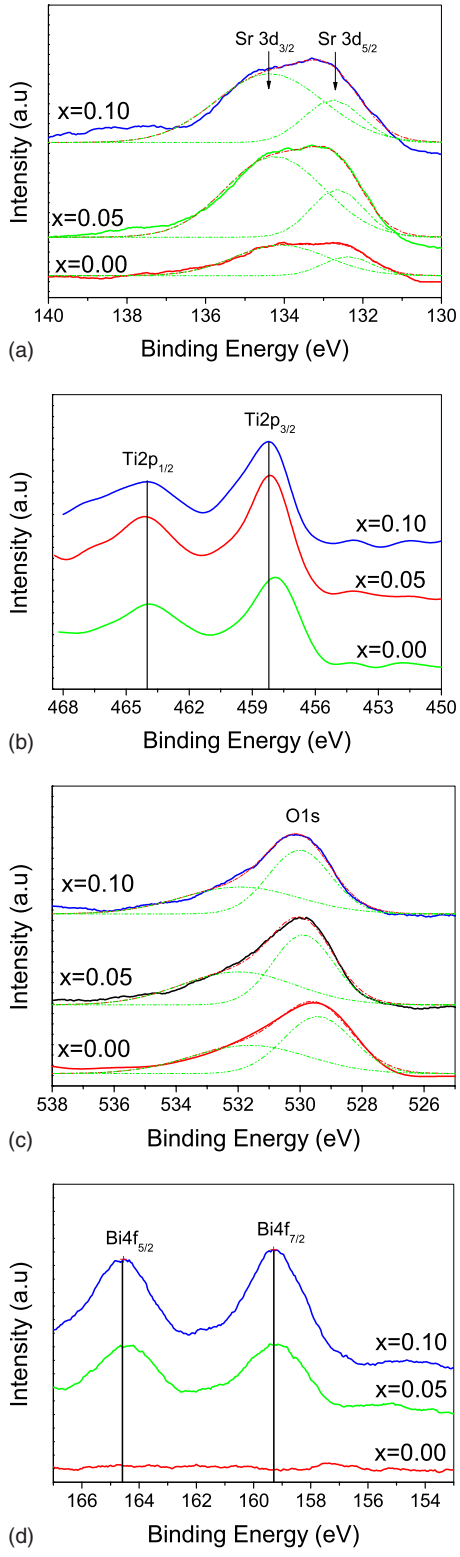

FIG. 2. (Color online) XPS narrow-scan spectra of the (a) Sr 3*d*, (b) Ti 3*p*, (c) O 1*s*, and (d) Bi 4*f* binding energy regions for the $(Sr_{1-1.5x}Bi_x)TiO_3$ (x=0,0.05,0.1) thin films.

The asymmetric narrow-scan spectra of O 1*s* are shown

TABLE I. Main peaks of each element for the reference and $Bi_xSr_{1-1.5x}TiO_3$ thin films (x=0,0.05,0.10) (C 1s standard, 284.8 eV) (Ref. 12).

Samples	Binding energy (eV)			
	Sr $3d_{5/2}$	Ti $2p_{3/2}$	O 1s	Bi $4f_{7/2}$
Bi_2O_3 [a]	···	···	529.80	158.60
$SrTiO_3$	132.29	457.90	530.02	···
$Bi_{0.05}Sr_{0.925}TiO_3$	131.65	457.62	529.91	159.30
$Bi_{0.10}Sr_{0.85}TiO_3$	131.60	457.55	529.43	159.30

[a]Reference 12.

in Fig. 2(c). The Gaussan-fitted subpeaks located at 530.02 and 532.00 eV for x=0.00, at 529.91 and 531.96 eV for x =0.05, and at 29.43 and 531.93 eV for x=0.10, are mainly ascribed to the metallic oxides and surface hydroxyl,[13] respectively. It can be seen that the binding energy of metallic oxides shifts to lower energy with the Bi doping.

Figure 2(d) shows that the Bi 4f doublet consists of two peaks at 159.30 and 164.58 eV, which are mainly identified as the signal from Bi($4f_{7/2}$)–O and Bi($4f_{5/2}$)–O bonds. Spin-orbit splitting energy of the pure Bi 4f doublet is 5.28 eV, indicating the chemical state of Bi is Bi^{3+}. There are no obvious shifts of Bi 4f peak for Bi doped thin films with different concentration of dopants.

According to XPS investigation, the electron-binding energies of the main peaks for the reference and each element were summarized and listed in Table I. It can be seen that there is a little shift to a lower energy spectrum in the main peak of Sr, Ti, and O for Bi-doped films, comparing to that of nondoped film.

In literature,[14,15] the chemical shifts in the electron-binding energies of the main peaks for the film may be related to the various electronegativity values for the elements. To estimate the ionicity of Bi–O, Sr–O, and Ti–O bonds for the $(Sr_{1-1.5x}Bi_x)TiO_3$ film, the fraction of ionicity (F_i) is given by[14,15]

$$F_i = 1 - \exp\left(-\frac{(EN_a - EN_c)^2}{4}\right), \quad (1)$$

where EN_a and EN_c are the anion and cation electronegativities, respectively.

According to the electronegativity values of Bi(2.02), Sr(0.95), Ti(1.54), and O(3.44), the F_i values for Bi–O, Sr–O, and Ti–O are 0.40, 0.79, and 0.60, respectively. It can be seen that the fraction of ionicity F_i (Bi–O) (0.40) is much smaller than F_i (Sr–O) (0.79), which indicating the bonding energy of (Bi, Sr)–O in the oxygen octahedron for Bi-doped films may be smaller than Sr–O bond for nondoped films. The shifts to lower energy of electron-binding main peaks of Sr and O confirm that there is a chemical reaction of substitution of Sr^{2+} by Bi^{3+} partially while the bismuth doped.

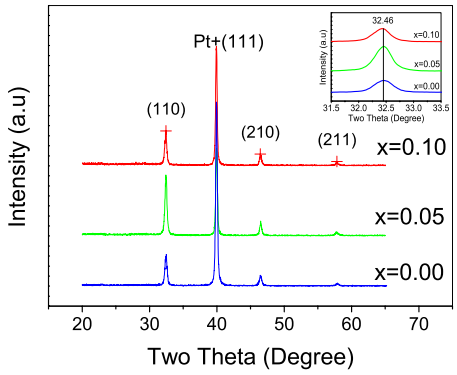

FIG. 3. (Color online) XRD patterns of BiST thin films annealed at 700 °C by RTA for 5 min. The indexes of perovskite phase are given in cubic notation. The inset shows the region of (110) reflection for BiST thin films.

Figure 3 shows XRD patterns of BiST thin films annealed at 700 °C by rapid thermal annealing (RTA) with 5 min for various Bi concentrations. The films show a cubic perovskite structure at random orientation with no other phase detected. The relative weak peak intensity and broader phenomena indicate that the size of crystal is small. The Bi concentration is in agreement with the nominal composition within the experimental error, and the distribution of Bi atoms is uniform. The results confirm that Bi ions are located at Sr sites.[10]

Figure 4 shows the AFM (2 Dimension) images on the surface of BiST thin films over a 5×5 μm^2 area by taping mode. The surface structures of BiST thin films are compact and smooth. The grain size of the aggregations is calculated and the value is about 100 nm in diameter. The rms roughness (root mean square roughness) of the films surface increases from 6.3 to 9.6 nm with increasing of doping content of bismuth accordingly.

SEM micrographs of the surface and cross section of BiST films are shown in Fig. 5. The films are dense and compact. The grain size increases with increase of Bi content, which is similar with the results of AFM images. The thickness of the films is 4.24, 3.96, and 4.09 μm for x

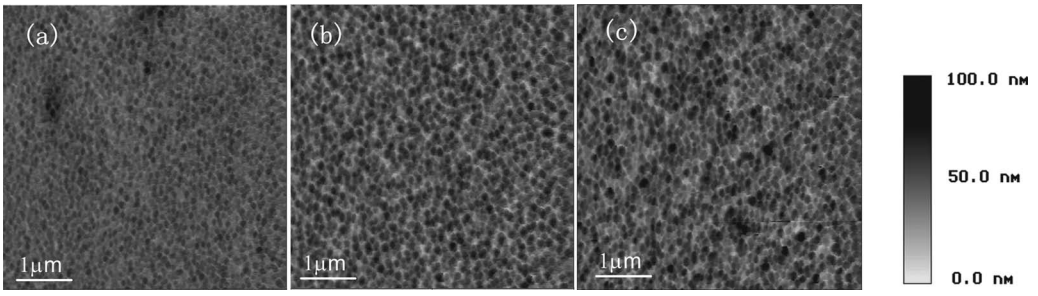

FIG. 4. AFM images of the surfaces of BiST thin films: (a) x=0.00, (b) x=0.05, and (c) x=0.10.

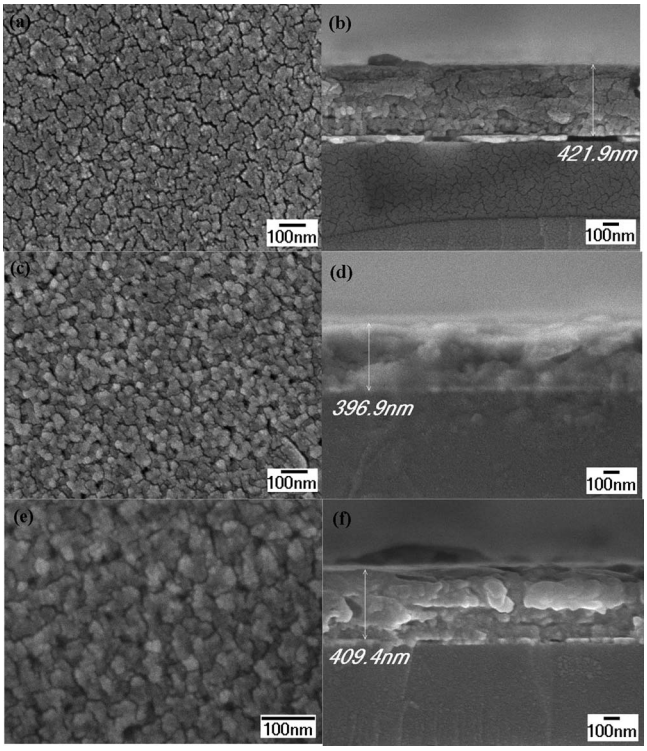

FIG. 5. Surface and cross-section SEM images of BiST thin films, [(a) and (b)] $x=0.00$, [(c) and (d)] $x=0.05$, and [(e) and (f)] $x=0.10$.

$=0.0$, 0.05, and 0.10, respectively. The results show that the introducing Bi ions resulted in the crystallization of the films accordingly.

The dielectric properties and capacitance-voltage (C-V) curves of the films are measured in a MFM configuration. The temperature dependence of dielectric properties and dielectric tunability has been studied as a function of the doping amount of bismuth. The tunability is determined by $\{(\varepsilon_{(0)}-\varepsilon_{(E\,\max)})/\varepsilon_{(0)}\}\times 100\%$, where $\varepsilon_{(0)}$ and $\varepsilon_{(E\,\max)}$ are the dielectric constants of BiST thin films at zero and maximum bias field, respectively. Figure 6 displays the dependence of dielectric constant (ε) as a function of applied bias electrical field (E) from $-E_{\max}$ to $E_{\max}$ as ε-E curves of the BiST thin films with different Bi content. The ε-E curves are measured from 1 to 500 kHz under a small oscillation signal of 50 mV at different frequency, which is considerably less than the coercive field of the material so that the ac field does not address the polarization state. It can be found that the dielectric constant changes little at low frequency and the dielectric constant of the films is significantly lower than that of the bulk ceramics.[7] The clamping effect in thin films due to the substrate constraint[16] and relative small grain size may result in a lower dielectric constant of the thin films.

The normalized dielectric constant and dielectric loss as a function of electrical fields with a cycling of sweeping bias voltage are shown in Fig. 7. The C-V plot represents butterflylike double peaks corresponding to the weak hysteresis loop and the dielectric properties keep stable at low frequency. As reported in literature,[1,6,17] $SrTiO_3$ and BiST are all in the paraelectric state at room temperature. In the case of BiST ceramics and $SrTiO_3$ films, shifts of T_c due to strains or defects are general phenomena and hysteresis loops of ε-E

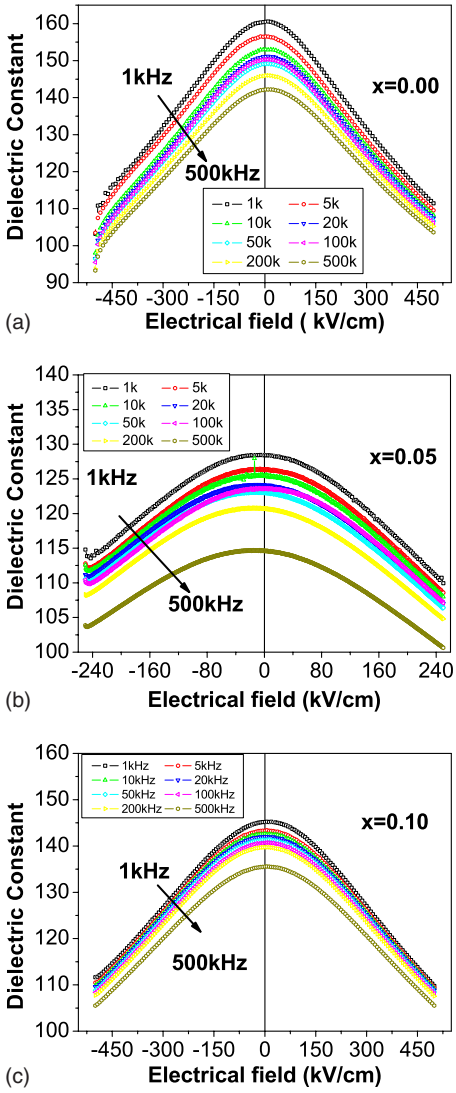

FIG. 6. (Color online) ε-E plots of $Bi_xSr_{1-1.5x}TiO_3$ thin films at different frequencies (a) $x=0.00$, (b) $x=0.05$, and (c) $x=0.10$.

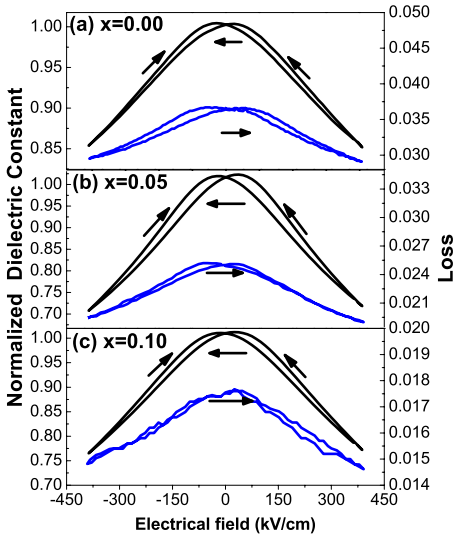

FIG. 7. (Color online) Normalized ε-E and dielectric loss plots of $Bi_xSr_{1-1.5x}TiO_3$ thin films at100 kHz.

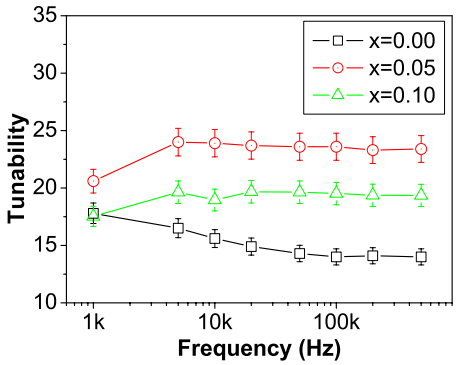

FIG. 8. (Color online) Tunability vs frequency plots of BiST thin films with different Bi doping content (bias field: 250 kV/cm).

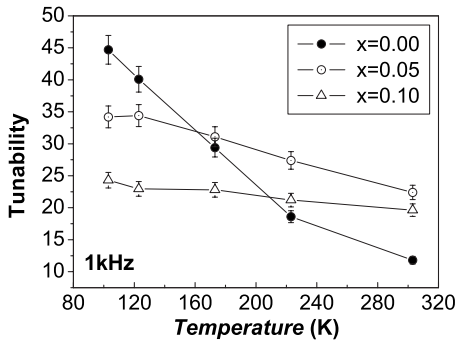

FIG. 9. Tunability vs temperature plots of BiST thin films with different Bi doping content (bias field: 250kV/cm).

characteristics are often observed.[2,5,6] According to the reports of Ang *et al.*[6] and our previous works,[17] the asymmetric ε-E property along the zero-bias voltage axes is attributed to the strong interaction between point defects and domain walls. When field is decreased after domains were fully orientated, point defects may drive domain walls back to the original positions. This equilibrium state may raise small signal dielectric constant up to its maximum. This confirms that the microdomains or polar clusters in Bi doped strontium titanate thin films can be changed by point defects, and then weak ferroelectric properties and dielectric tunable can be observed.

From the results illustrated in Fig. 7, it shows that the dielectric loss decreases with increasing Bi doping content. Yamada *et al.*[18] has reported that the subtraction of the intrinsic loss contribution from the measurement value of the loss tangent of the films in the paraelectric phase under dc bias fields can be effective in evaluating the extrinsic loss contribution of the films. Moreover, according to the results of BiST ceramics and Cr-doped BST films reported in literature,[19,20] the decrease of dielectric loss is attributed to the oxygen-vacancy related relaxations. The influence of oxygen vacancies is lowered due to the doped Bi^{3+} ions acting as acceptors in the films to weaken the influence on the quantum fluctuations from oxygen vacancies.

The tunability of BiST films with different Bi doping content as a function of the frequency are shown in Fig. 8. It can be seen that the tunability of the films change little from 1 to 500 kHz. These results also show a clear trend improved film dielectric tunability by doping small concentration of bismuth in $SrTiO_3$ thin film, for the same bias field. The tunability of the films for $x=0.05$ is relatively higher than that for $x=0.1$, and the tunability of the films for $x=0.1$ is higher than that for $x=0$ also. The temperature dependence of the tunability of BiST thin films is measured and the plots are shown in Fig. 9. It can be found that the tunability decreases, for $x=0$, 0.05, and 0.10, as temperature increases from 100 K to room temperature at 1 kHz. When the temperature is lower than 160 K, the higher tunability is observed for the films with $x=0.0$ and the lower is observed for $x=0.10$. On the other hand, when the temperature is higher than 210 K, the higher tunability is observed for the films with $x=0.05$ and the lower is observed for $x=0$. The tunability of Bi doped $SrTiO_3$ films for $x=0.05$ is larger than that for $x=0.10$ over the whole temperature range, which is similar with the results of Bi-doped $SrTiO_3$ ceramics.

According to the phenomenological theory of Devonshire and the simplified expression proposed by Johnson,[21,22] the equation can be written as

$$\frac{\varepsilon_r(T,0)}{\varepsilon_r(T,E)} = \{1 + [\varepsilon_0 \varepsilon_r(T,0)]^3 B(T) E^2\}^{1/3}, \tag{2}$$

where the left is the tunability ratio, ε_0 is the vacuum dielectric constant, $\varepsilon_r(T,0)$ is the relative dielectric permittivity at temperature T without dc bias, $B(T)$ is the phenomenological coefficient of the fourth power of polarization and it has a weak relation with the temperature, and E is the external dc bias field. So the tunability is directly proportional to $\varepsilon_r(T,0)$.[21,22]

As reported in literature,[7,11] the coexistence of two different set of dielectric peaks with different physical characteristics in Bi doped $SrTiO_3$ can be observed, the oxygen vacancies related relaxations at higher temperature and ferroelectric relaxor mode at lower temperature, while the doped Bi concentration is lower than 10%. At high temperature (160–400 K), the dielectric permittivity has a tight relation with the strengths of the oxygen-vacancy related relaxation. On the other hand, the dielectric permittivity may be mainly attributed to the ferroelectric relaxor mode relaxation induced by Bi^{3+} ions substitutions for Sr^{2+} at lower temperature (below 160 K).

As we know that for the perovskite structure oxidation materials containing titanate, the oxygen vancancies can be easily created by loss of oxygen from the crystal lattice at low oxygen partial pressure or high annealing temperature for Bi-doped $SrTiO_3$.[7] The first ionization of the oxygen vacancies will create the conducting electrons[7] and the equations can be written as

$$O_o \Leftrightarrow V_O + \tfrac{1}{2}O_2, \tag{3}$$

$$V_O \Leftrightarrow V_O^{\bullet} + e'. \tag{4}$$

These electrons may be bonded or trapped by Ti^{4+} or oxygen vacancies. The contribution of the conduction electrons (or holes or protons) to dielectric polarization has been reported as an "electron relaxation-mode coupling model" to explain the very high permittivity in Nb-doped BT by Maglione and Belkaoumi.[23] The polarization can be greatly enhanced by

the interaction of the electrons and the dielectric relaxation process, even with low concentration of the dipoles, and the system can exhibit a very high permittivity. In Bi-doped $SrTiO_3$ system, the permittivity of the material depends on the concentration of the electrons and the contribution of the combination effects of the reorientation of the off-center Bi and Ti ions coupling with the conducting electrons.[7] When the Bi concentration is low, higher concentration of the intrinsic oxygen vacancies and electrons are achieved. This results in the high permittivity step in the materials. While the Bi concentration is larger than 0.04, the concentration of both oxygen vacancies and electrons become small with the increase of Bi concentration, and hence, dielectric permittivity and tunability decrease accordingly.[7,11]

According to the previous research,[6,24,25] Bi^{3+} ions substitutions for Sr^{2+} in $SrTiO_3$ are located at off-center positions and *A*-site vacancies (V''_{Sr}) also appear to compensate the charge imbalance arising from the substitution, then Bi^{3+}-V''_{Sr} dipolar defect is formed, which is a highly polarizable ion tending to induce polar clusters. These dipoles are dispersing at random locations in the host lattice, which form polar nanoregions, and finally play a destructive role in the primary long-range paraelectric order structure. In the very dilute limit, each polar domain behaves as a noninteracting dipolar entity. With increasing Bi^{3+} concentration, the concentration of impurity induced polar nanoregions increase accordingly. The interactions among these regions become remarkable and the dielectric increases. When $x>0.04$, the interaction between the polar clusters is strong enough, and the ferroelectric relaxor mode relaxation dominates. With the increase of Bi concentration, the peak of relaxation shifts to high temperature and the dielectric permittivity decreases accordingly.[6]

Above all, the dielectric behavior and dielectric tunability should be attributed to the sum of ferroelectric relaxor relaxation and the combination effects of the reorientation of the off-center Bi and Ti ions coupling with the conducting electrons induced by oxygen vacancies related relaxation. When the Bi concentration is lager than 0.04, the dielectric tunability decreases with the increase of Bi content. It is in agreement with our experimental results.

IV. CONCLUSION

Dense and crack-free bismuth doped strontium titanate $[(Sr_{1-1.5x}Bi_x)TiO_3, x=0.0, 0.05, 0.1]$ thin films with a perovskite structure have been successfully prepared by a sol-gel process. With the addition of Bi dopants lower than 10%, crystallization of the films being improved, higher tunability and good dielectric properties have been obtained for BiST thin films. The dielectric loss decreases with the increase of doping content accordingly. The interesting dielectric behavior and tunability should be attributed to the sum of ferroelectric relaxor relaxation induced by Bi^{3+} ions substitutions for Sr^{2+} in $SrTiO_3$ and the combination effects of the reorientation of the off-center Bi and Ti ions coupling with the conducting electrons created by oxygen vacancies related relaxation.

ACKNOWLEDGMENTS

Support for this research from the National Natural Sciences Foundation of China under Grant Nos. 50602034 and U0634006 are gratefully acknowledged.

[1] K. A. Muller and H. Burkhard, Phys. Rev. B **19**, 3593 (1979).
[2] J. H. Haeni, P. Irvin, W. Chang, R. Uecker, P. Reiche, Y. L. Li, S. Choudhury, W. Tian, M. E. Hawley, B. Craigo, A. K. Tagantsev, X. Q. Pan, S. K. Streiffer, L. Q. Chen, S. W. Kirchoefer, J. Levy, and D. G. Schlom, Nature (London) **430**, 758 (2004).
[3] J. G. Bednorz and K. A. Muller, Phys. Rev. Lett. **52**, 2289 (1984).
[4] V. A. Isupov, Fiz. Tverd. Tela (St. Petersburg) **47**, 2152 (2005); [Phys. Solid State **47**, 2243 (2005)].
[5] C. Ang, Z. Yu, and L. Cross, Phys. Rev. B **62**, 228 (2000).
[6] C. Ang, Z. Yu, P. Lunkenheimer, J. Hemberger, and A. Loid, Phys. Rev. B **59**, 6661 (1999); **59**, 6670 (1999).
[7] C. Ang, Z. Yu, and L. Cross, Phys. Rev. B **62**, 228 (2000).
[8] C. Ang and Z. Yu, J. Appl. Phys. **91**, 1487 (2002).
[9] C. Ang, Z. Yu, P. M. Vilarinho, and J. L. Baptista, Phys. Rev. B **57**, 7403 (1998).
[10] C. Ang and Z. Yu, Phys. Rev. B **61**, 11363 (2000).
[11] W. Chen, X. Yao, and X. Y. Wei, Appl. Phys. Lett. **90**, 182902 (2007).
[12] C. D. Wagner, W. M. Riggs, L. E.Davis, *Handbook of X-ray Photoelectron Spectroscopy* (Perking-Elmer Corporation: Physical Electronics Division, Eden Prairie, MN, 1979).
[13] Z. L. Liu, B. Guo, L. Hong, and H. Jiang, J. Phys. Chem. Solids **66**, 161 (2005).
[14] Z. Quan, W. Liu, H. Hu, S. Xu, B. Sebo, G. Fang, M. Y. Li, and X. Z. Zhao, J. Appl. Phys. **104**, 084106 (2008).
[15] D. R. Askeland, *The Science and Engineering of Materials* (PWS, Boston, 1994).
[16] B. Su, J. E. Holmes, C. Meggs, and T. W. Button, J. Eur. Ceram. Soc. **23**, 2699 (2003).
[17] X. Y. Wei, Y. J. Feng, L. M. Hang, S. Xia, L. Jin, and X. Yao, Mater. Sci. Eng., B **120**, 64 (2005).
[18] T. Yamada, K. F. Astafiev, V. O. Sherman, A. K. Tagantsev, D. Su, P. Muralt, and N. Setter, J. Appl. Phys. **98**, 054105 (2005).
[19] S. W. Yu, J. Cheng, R. Li, W. C. Zhu, and Z. Y. Meng, IEEE Trans. Ultrason. Ferroelectr. Freq. Control **55**, 1029 (2008).
[20] L. C. Walters and R. E. Grace, J. Phys. Chem. Solids **28**, 239 (1967).
[21] K. M. Johnson, J. Appl. Phys. **33**, 2826 (1962).
[22] A. Outzourhit, J. U. Trefny, T. Kito, B. Yarar, A. Naziripour, and A. M. Hermann, Thin Solid Films **259**, 218 (1995).
[23] M. Maglione and M. Belkaoumi, Phys. Rev. B **45**, 2029 (1992).
[24] L. Zhou, P. M. Vilarinho, and J. L. Baptista, J. Eur. Ceram. Soc. **21**, 531 (2001).
[25] W. Chen, X. Yao, and X. Y. Wei, J. Mater. Sci. **43**, 1144 (2008).